

DETC2003/VIB-48441

COMPONENT MODE SYNTHESIS USING NONLINEAR NORMAL MODES

Polarit Apiwattanalunggarn
Steven W. Shaw

Department of Mechanical Engineering
Michigan State University
East Lansing, Michigan 48824-1226
Email: apiwatta@egr.msu.edu, shaw@egr.msu.edu

Christophe Pierre*

Department of Mechanical Engineering
University of Michigan
Ann Arbor, Michigan 48109-2125
Email: pierre@umich.edu

ABSTRACT

This paper describes a methodology for developing reduced-order dynamic models of nonlinear structural systems that are composed of an assembly of component structures. The approach is a nonlinear extension of the fixed-interface component mode synthesis technique developed for linear structures by Hurty and modified by Craig and Bampton. Specifically, the case of nonlinear substructures is handled by using fixed-interface nonlinear normal modes. These normal modes are constructed for the various substructures using an invariant manifold approach, and are then coupled through the traditional linear constraint modes (i.e., the static deformation shapes produced by unit interface motions). A simple system is used to demonstrate the proof of concept and show the effectiveness of the proposed procedure. Simulations are performed to show that the reduced-order model obtained from the proposed procedure outperforms the reduced-order model obtained from the classical fixed-interface linear component mode synthesis approach. Moreover, the proposed method is readily applicable to large-scale nonlinear structural systems.

INTRODUCTION

Many complex structures are composed of several relatively simple substructures that are assembled together. This occurs in trusses, bladed-disk assemblies in turbine rotors, aerospace and ground vehicles, and many other applications. In such cases it

is convenient to develop a dynamic model for the overall structure by taking advantage of the dynamic properties of the substructures. Component Mode Synthesis (CMS) was developed with those ideas, in order to synthesize models that are described in terms of the component structures and to take advantage of model size reduction carried out at the substructure level. There are two general types of CMS methods; they are known as the fixed-interface and the free-interface approaches. The fixed-interface CMS technique, developed by Hurty ([1], [2]) and simplified by Craig and Bampton ([3]), is widely used, since the reduction procedure is straightforward and typically produces highly accurate models with few component modes ([4]). An extensive review on CMS can be found in [5]. CMS-type methods are well developed for linear structural models and they have been used extensively, especially in the aerospace industry ([6], [7], [8], [9], [10], and etc.).

The finite element (FE) method is a versatile tool for modeling complex structures, and is used in CMS to model and characterize the substructures. Generally, accurate models of component structures require a large number of FE degrees of freedom (DOF). For linear systems, model reduction can be achieved using linear modal analysis, wherein one simply truncates the higher modes of free vibration. In fact, this is how one carries out model size reduction for the substructures in linear CMS. However, the dynamic analysis (e.g., the determination of natural frequencies, mode shapes, time responses) of such structures can require considerable computational effort, and this is especially the case for nonlinear structures ([11]).

*Address all correspondence to this author.

The difficult issue of model size reduction for nonlinear structures continues to be a major challenge for computational vibration analysis. For relatively simple systems one can use nonlinear normal modes (NNMs) for this task. For example, Shaw and Pierre have developed systematic procedures to obtain reduced-order models (ROM) via NNMs using invariant manifolds ([12], [13], and [14]). Asymptotic series were initially used to approximate the geometry of the invariant manifold, and this approach was applied to the study of a variety of systems, such as a nonlinear rotating Euler-Bernoulli Beam ([15]). Pesheck *et al.* developed a numerically-based Galerkin approach to calculate the geometry of the NNM invariant manifolds out to large amplitudes of vibration ([16]). These procedures can be used for quite general nonlinearities over a wide range of amplitude, and they have been applied to many systems, including the rotating beam ([17]). Recently, these methods have been shown to be applicable in conjunction with nonlinear FE models ([18]), which opens a new frontier for their application to more complex nonlinear structural systems.

The present paper describes recent research that is aimed at extending the fixed-interface linear CMS method to nonlinear structures by making use of the fixed-interface NNMs of the component structures. By synthesizing the reduced-order representations of the substructures, one can obtain accurate low-order models of nonlinear structures that are composed of assemblies of substructures.

The paper is outlined as follows. We first review the development of NNMs, as needed for the individual substructures. The associated invariant manifold equations, parameterized by modal position and velocity, are formulated, and a numerical collocation method is presented that allows one to obtain the solution of the NNM invariant manifold. Then, the procedures for fixed-interface nonlinear component mode synthesis are described. A five-DOF spring-mass system is used as an example to demonstrate the method, and some conclusions are drawn to close the paper.

1 FORMULATION OF INVARIANT MANIFOLD PARAMETERIZED BY MODAL POSITION AND VELOCITY

We begin with a general discrete representation of the vibrations of a nonlinear structural system, obtained either by a finite element model followed by linear modal expansion, or by a Rayleigh-Ritz approach. We assume that the system at linear order is undamped. This assumption greatly simplifies the problem, but can be relaxed in principle. In this case, the equations of motion for an Q -DOF system are uncoupled at linear order and can be expressed in the form:

$$\mathbf{I} \ddot{\boldsymbol{\eta}} + \Lambda \boldsymbol{\eta} = \mathbf{f}(\boldsymbol{\eta}, \dot{\boldsymbol{\eta}}) \quad (1)$$

where \mathbf{I} is the identity matrix, Λ the diagonal matrix of squared linear frequencies, $\mathbf{f}(\boldsymbol{\eta}, \dot{\boldsymbol{\eta}})$ a vector of nonlinear forces, $\boldsymbol{\eta}$ the modal position vector, and $\dot{\boldsymbol{\eta}}$ the modal velocity vector. The component form of equation (1) is given by

$$\ddot{\eta}_i + \omega_i^2 \eta_i = f_i(\eta_j, \dot{\eta}_j) \quad (2)$$

$$\text{for } i, j = 1, 2, 3, \dots, Q$$

where ω_i is the linear free vibration natural frequency of mode i and Q is the number of retained linear modes.

In order to search for a particular individual NNM, it is assumed that the NNM manifold is parameterized by a single modal position-velocity pair corresponding to the mode of interest, referred to as the master mode. This is accomplished by using the fact that for a NNM response all of the remaining modal positions and velocities are slaved (constrained) to this master mode. For the k th nonlinear mode, we take $u_k = \eta_k$, and $v_k = \dot{\eta}_k$ as the master states. The remaining slave states are expressed as

$$\eta_i = X_i(u_k, v_k) = X_i(\eta_k, \dot{\eta}_k) \quad (3)$$

$$\dot{\eta}_i = Y_i(u_k, v_k) = Y_i(\eta_k, \dot{\eta}_k) \quad (4)$$

$$\text{for } i = 1, 2, 3, \dots, Q, i \neq k.$$

Equations (3) and (4) constitute a set of constraint equations that are to be determined. The constraint functions in equations (3) and (4) are obtained by an invariant manifold procedure that generates equations that can be solved for the unknown constraint relations. The process begins by taking a time derivative of the constraint equations, yielding

$$\dot{\eta}_i = \frac{\partial X_i}{\partial u_k} \dot{u}_k + \frac{\partial X_i}{\partial v_k} \dot{v}_k \quad (5)$$

$$\ddot{\eta}_i = \frac{\partial Y_i}{\partial u_k} \dot{u}_k + \frac{\partial Y_i}{\partial v_k} \dot{v}_k \quad (6)$$

$$\text{for } i = 1, 2, 3, \dots, Q, i \neq k.$$

The time dependence in these equations is eliminated by using the following relations: $\dot{u}_k = v_k$, $\dot{v}_k = \ddot{\eta}_k = -\omega_k^2 \eta_k + f_k(\eta_j, \dot{\eta}_j)$. Then, the constraints (equations (3) and (4)) are substituted in the resulting expression everywhere in place of the

slave state variables, resulting in a set of partial differential equations for the functions $(X_i(u_k, v_k), Y_i(u_k, v_k))$. This set of $2N - 2$, time-independent, partial differential equations govern the geometry of the k th manifold, and are given by

$$Y_i = \frac{\partial X_i}{\partial u_k} v_k + \frac{\partial X_i}{\partial v_k} (-\omega_k^2 u_k + f_k(X_j, Y_j, u_k, v_k)) \quad (7)$$

$$-\omega_i^2 X_i + f_i(X_j, Y_j, u_k, v_k) = \frac{\partial Y_i}{\partial u_k} v_k + \frac{\partial Y_i}{\partial v_k} (-\omega_k^2 u_k + f_k(X_j, Y_j, u_k, v_k)) \quad (8)$$

for $i, j = 1, 2, 3, \dots, Q, i, j \neq k$.

These equations are not solvable in closed form (except in very special cases) and methods for obtaining approximate solutions for X_i and Y_i are described in the next section.

2 INVARIANT-MANIFOLD SOLUTION

Asymptotic expansions can be used to obtain approximate solutions of the invariant manifold equations, equations (7) and (8), for smooth nonlinearities, but such solutions are only locally valid ([12], [13]). Numerical Galerkin-based solutions have also been developed, wherein one can utilize either local or global basis functions to describe the invariant manifold ([16]). In this work we employ a Galerkin-based procedure that relies on a patchwork of local solutions to obtain a solution that is valid over the entire domain $u_k \in [-U_b, U_b]$ and $v_k \in [-V_b, V_b]$.

We describe the development of the method for a local domain described by $u_k^e \in [-u_b, u_b]$ and $v_k^e \in [-v_b, v_b]$. Once this procedure has been developed, it can be applied to each patch, and the final result is obtained by collecting the results for all patches such that the entire domain is covered. The relations between the coordinates in the global domain (u_k, v_k) and those in the local domain (u_k^e, v_k^e) are given by

$$u_k = d_u + u_k^e, \quad (9)$$

$$v_k = d_v + v_k^e, \quad (10)$$

$$\text{where } d_u = -U_b + \left(\frac{2U_b}{N_u^e}\right)(e_u - 1) + u_b, \quad (11)$$

$$\text{and } d_v = -V_b + \left(\frac{2V_b}{N_v^e}\right)(e_v - 1) + v_b, \quad (12)$$

where e_u and e_v are the patch indices in the u_k and v_k directions, respectively, and N_u^e and N_v^e are the number of patches used in the u_k and v_k directions, respectively.

Substituting equations (9) and (10) into equations (7) and (8), the partial differential equations governing the geometry of the k th manifold in the local coordinates (u_k^e, v_k^e) are given by:

$$Y_i = \frac{\partial X_i}{\partial u_k^e} (d_v + v_k^e) + \frac{\partial X_i}{\partial v_k^e} (-\omega_k^2 (d_u + u_k^e) + f_k(X_j, Y_j, d_u + u_k^e, d_v + v_k^e)) \quad (13)$$

$$-\omega_i^2 X_i + f_i(X_j, Y_j, d_u + u_k^e, d_v + v_k^e) = \frac{\partial Y_i}{\partial u_k^e} (d_v + v_k^e)$$

$$+ \frac{\partial Y_i}{\partial v_k^e} (-\omega_k^2 (d_u + u_k^e) + f_k(X_j, Y_j, d_u + u_k^e, d_v + v_k^e)) \quad (14)$$

for $i, j = 1, 2, 3, \dots, Q, i, j \neq k$.

The solution of equations (13) and (14) on the local domain is obtained by expanding (X_i, Y_i) in terms of basis functions as:

$$X_i(u_k^e, v_k^e) = \sum_{l=1}^{N_{p,u}} \sum_{m=1}^{N_{p,v}} C_i^{l,m} LM_{l,m}(u_k^e, v_k^e) \quad (15)$$

$$Y_i(u_k^e, v_k^e) = \sum_{l=1}^{N_{p,u}} \sum_{m=1}^{N_{p,v}} D_i^{l,m} LM_{l,m}(u_k^e, v_k^e), \quad (16)$$

$$\text{where } LM_{l,m}(u_k^e, v_k^e) = T_{l-1}(u_k^e/u_b) \times T_{m-1}(v_k^e/v_b), \quad (17)$$

where $T_{l-1}(x)$ and $T_{m-1}(x)$ are standard Chebyshev polynomials defined over $x \in [-1, +1]$, and the C 's and D 's are the to-be-determined expansion coefficients. Equations (15) and (16) are substituted into the local manifold-governing equations, equations (13) and (14). Normally, each of the resulting equations is projected onto the basis functions, but here we employ a collocation method, which is computationally more efficient yet retains very good accuracy. This is carried out by projection of the equations onto *Dirac delta functions* in the local master coordinates over the local domain, yielding

$$0 = \int_{u_k^e, v_k^e} \delta(u_k^e - u_{k,p}^e, v_k^e - v_{k,q}^e) \left[- \sum_{l,m} D_i^{l,m} LM_{l,m} + \sum_{l,m} C_i^{l,m} (d_v + v_k^e) \frac{\partial LM_{l,m}}{\partial u_k^e} \right]$$

$$+ \sum_{l,m} C_i^{l,m} \frac{\partial LM_{l,m}}{\partial v_k^e} (-\omega_k^2 (d_u + u_k^e) + f_k) \Big] du_k^e dv_k^e \quad (18)$$

$$0 = \int_{u_k^e, v_k^e} \delta(u_k^e - u_{k,p}^e, v_k^e - v_{k,q}^e) \left[\omega_i^2 \sum_{l,m} C_i^{l,m} LM_{l,m} - f_i + \sum_{l,m} D_i^{l,m} (d_v + v_k^e) \frac{\partial LM_{l,m}}{\partial u_k^e} + \sum_{l,m} D_i^{l,m} \frac{\partial LM_{l,m}}{\partial v_k^e} (-\omega_k^2 (d_u + u_k^e) + f_k) \right] du_k^e dv_k^e \quad (19)$$

for $i = 1, 2, 3, \dots, Q, i \neq k$;

$p = 1, \dots, N_{p,u}$;

$q = 1, \dots, N_{p,v}$,

where $(u_{k,p}^e, v_{k,q}^e) \in [-u_b, u_b] \times [-v_b, v_b]$ are the collocation points. Equations (18) and (19) constitute a set of $2(Q-1) \times N_{p,u} \times N_{p,v}$ nonlinear equations in the C 's and D 's. Note that there are $N_u^e \times N_v^e$ sets of C 's and D 's. However, if the system is conservative and the nonlinear terms are functions of solely the modal positions, then only $0.25 \times N_u^e \times N_v^e$ sets of C 's and D 's need to be solved for, and the remaining coefficients can be generated using symmetries in the solution. Once all of the expansion coefficients are obtained, the X 's and Y 's, which describe the slaved modes, are known functions of the master states (u_k^e, v_k^e) . For $i = k$, these known functions are used to express f_k in equation (2) in terms of only u_k^e and v_k^e , rendering a single-DOF oscillator as the reduced-order-model for the k^{th} NNM.

3 FIXED-INTERFACE NONLINEAR COMPONENT MODE SYNTHESIS

In this section, we extend the concept of the fixed-interface CMS of Craig and Bampton ([3]) by making use of the fixed-interface NNMs instead of the fixed-interface linear normal modes (LNMs). First, the nonlinear structural system is partitioned into two component structures. Then, fixed-interface dynamic representations of both substructures are constructed, where the nonlinear models are expressed in terms of fixed-interface LNMs. These substructure models are then reduced using the NNM constraint relations, and subsequently synthesized with linear constraint modes to produce a ROM that describes the dynamics of the combined structure.

3.1 System Representation in Physical Coordinates

Consider a structure that is partitioned into two substructures, denoted by α and β . The equations of motion of the substructures in physical coordinates can be written separately, along with appropriate conditions on the common junction coordinates, as follows:

$$\begin{bmatrix} \mathbf{M}_{\Pi} & \mathbf{M}_{\text{IJ}} \\ \mathbf{M}_{\text{JI}} & \mathbf{M}_{\text{JJ}} \end{bmatrix}^\alpha \begin{bmatrix} \ddot{\mathbf{X}}_{\text{I}} \\ \ddot{\mathbf{X}}_{\text{J}} \end{bmatrix}^\alpha + \begin{bmatrix} \mathbf{K}_{\Pi} & \mathbf{K}_{\text{IJ}} \\ \mathbf{K}_{\text{JI}} & \mathbf{K}_{\text{JJ}} \end{bmatrix}^\alpha \begin{bmatrix} \mathbf{X}_{\text{I}} \\ \mathbf{X}_{\text{J}} \end{bmatrix}^\alpha \quad (20)$$

$$+ \begin{bmatrix} \mathbf{G}_{\text{I}}(\mathbf{X}) \\ \mathbf{G}_{\text{J}}(\mathbf{X}) \end{bmatrix}^\alpha = \begin{bmatrix} \mathbf{0} \\ \mathbf{F}_{\text{J}} \end{bmatrix}^\alpha$$

$$\begin{bmatrix} \mathbf{M}_{\Pi} & \mathbf{M}_{\text{IJ}} \\ \mathbf{M}_{\text{JI}} & \mathbf{M}_{\text{JJ}} \end{bmatrix}^\beta \begin{bmatrix} \ddot{\mathbf{X}}_{\text{I}} \\ \ddot{\mathbf{X}}_{\text{J}} \end{bmatrix}^\beta + \begin{bmatrix} \mathbf{K}_{\Pi} & \mathbf{K}_{\text{IJ}} \\ \mathbf{K}_{\text{JI}} & \mathbf{K}_{\text{JJ}} \end{bmatrix}^\beta \begin{bmatrix} \mathbf{X}_{\text{I}} \\ \mathbf{X}_{\text{J}} \end{bmatrix}^\beta \quad (21)$$

$$+ \begin{bmatrix} \mathbf{G}_{\text{I}}(\mathbf{X}) \\ \mathbf{G}_{\text{J}}(\mathbf{X}) \end{bmatrix}^\beta = \begin{bmatrix} \mathbf{0} \\ \mathbf{F}_{\text{J}} \end{bmatrix}^\beta,$$

with junction boundary conditions on displacements and forces:

$$\mathbf{X}_{\text{J}}^\alpha = \mathbf{X}_{\text{J}}^\beta, \quad (22)$$

$$\mathbf{F}_{\text{J}}^\alpha + \mathbf{F}_{\text{J}}^\beta = \mathbf{0}, \quad (23)$$

where $(\cdot)^\alpha$ denotes quantities associated with substructure α , and all terms defined below have their $(\cdot)^\beta$ counterparts. The vector \mathbf{X}^α contains all coordinates for the α substructure and has dimension N^α , $\mathbf{X}_{\text{I}}^\alpha$ is the vector of interior (non-interface) physical coordinates of dimension n_{I}^α , and $\mathbf{X}_{\text{J}}^\alpha$ is the vector of junction (interface) physical coordinates of dimension n_{C} . $\mathbf{G}_{\text{I}}^\alpha$ is a vector of the nonlinear forces associated with the $\mathbf{X}_{\text{I}}^\alpha$ equations, $\mathbf{G}_{\text{J}}^\alpha$ is the vector of nonlinear forces associated with the $\mathbf{X}_{\text{J}}^\alpha$ equations, and $\mathbf{F}_{\text{J}}^\alpha$ is the vector of reaction forces from substructure β applied on substructure α . \mathbf{M}_{Π}^α , \mathbf{K}_{Π}^α , etc., are mass and stiffness matrices, respectively, defined in an obvious manner.

3.2 System Representation in Linear Modal Coordinates

In this section, the (typically) large number of physical coordinates for each substructure is first reduced to a smaller (yet still possibly large) number of coordinates by truncating using the substructures' fixed-interface linear modes; note that this is the first place where an approximation is made. The physical coordinates of substructures α and β are transformed into a truncated set of fixed-interface linear modal coordinates using the following coordinate transformations:

$$\mathbf{X}^\alpha = \Psi^\alpha \eta^\alpha = \begin{bmatrix} \Phi_{\text{N}}^\alpha & \Psi_{\text{C}}^\alpha \end{bmatrix} \begin{bmatrix} \eta_{\text{N}}^\alpha \\ \eta_{\text{C}}^\alpha \end{bmatrix} \quad (24)$$

$$\mathbf{X}^\beta = \Psi^\beta \eta^\beta = \begin{bmatrix} \Phi_N^\beta & \Psi_C^\beta \end{bmatrix} \begin{bmatrix} \eta_N^\beta \\ \eta_C^\beta \end{bmatrix}, \quad (25)$$

where Φ_N^α is the $N^\alpha \times n^\alpha$ matrix of retained fixed-interface linear normal modes, η_N^α is the vector of retained fixed-interface linear modal coordinates (of dimension n^α), Ψ_C^α is the $N^\alpha \times n_C$ matrix of linear constraint modes, η_C^α is the vector (of dimension n_C) of linear constraint modal coordinates, and similar terms are defined for substructure β . The procedures for calculating the retained fixed-interface linear normal modes and the linear constraint modes will be described subsequently. Note that at this step, the dimension of the system of equations for substructure α has been reduced from ($N^\alpha = n_I^\alpha + n_C$) to ($n^\alpha + n_C$) with $n^\alpha \ll n_I^\alpha$, and the same is true for substructure β .

3.2.1 Fixed-Interface Linear and Nonlinear Normal Modes. The concept of fixed-interface linear CMS of Craig and Bampton ([3]) is extended by making use of the fixed-interface NNMs in place of the fixed-interface LNMs. Since the procedures for substructures α and β are the same, these superscripts will be omitted from the development.

Consider equations (20) and (21) with $\mathbf{X}_J = \mathbf{0}$, that is, with the interface fixed. This yields

$$\mathbf{M}_{II} \ddot{\mathbf{X}}_I + \mathbf{K}_{II} \mathbf{X}_I + \mathbf{G}_I(\mathbf{X}_I, \mathbf{X}_J = \mathbf{0}) = \mathbf{0}. \quad (26)$$

Using standard linear modal analysis (with the modes obtained for $\mathbf{G}_I = \mathbf{0}$), we obtain the normalized fixed-interface linear modal matrix associated with the interior physical coordinates Φ_{IN} (of dimension $n_I \times n$, where $n \ll n_I$). Then, the retained fixed-interface linear modal matrix Φ_N is defined as

$$\Phi_N = \begin{bmatrix} \Phi_{IN} \\ \mathbf{0} \end{bmatrix}. \quad (27)$$

The nonlinear equations of motion (26) are then transformed into fixed-interface linear modal coordinates using the following coordinate transformation:

$$\mathbf{X}_I = \Phi_{IN} \eta_N. \quad (28)$$

This yields the fixed interface nonlinear equations of motion expressed in fixed-interface linear modal coordinates, as follows:

$$\mathbf{I}_{NN} \ddot{\eta}_N + \Lambda_{NN} \dot{\eta}_N + \tilde{\mathbf{G}}_N(\eta_N) = \mathbf{0}. \quad (29)$$

This fixed-interface model is still relatively large and is to be ultimately reduced to a single DOF using the nonlinear modal reduction procedure described in sections 1 and 2. Note that in terms of matching notation, the function $\tilde{\mathbf{G}}_N$ and dimension n here are $-\mathbf{f}$ and Q , respectively, in those sections. The NNM reduction provides the constraint relations between the slaved states and the master states of the k^{th} fixed-interface NNM for a substructure, and can be expressed as follows:

$$\eta_i^N = X_i(\eta_k^N, \dot{\eta}_k^N) \quad (30)$$

$$\dot{\eta}_i^N = Y_i(\eta_k^N, \dot{\eta}_k^N) \quad (31)$$

for $i = 1, 2, 3, \dots, n, i \neq k$.

At this stage we have single mode nonlinear models for the substructures, based on a fixed interface model. We now turn to the procedure for coupling these component structure models to one another through the interface.

3.2.2 Linear Constraint Modes. The definition of a linear constraint mode from [3] is adopted here. It is defined by statically imposing a unit displacement on one physical coordinate of the set of junction coordinates and zero displacements on the remaining coordinates of the set. This procedure is applied consecutively to all junction coordinates. Again, this process is the same for the α and β substructures, and therefore these superscripts are omitted. The collection of linear constraint modes is obtained from

$$\Psi_C = \begin{bmatrix} \Psi_{IC} \\ \mathbf{I}_{JC} \end{bmatrix} = \begin{bmatrix} -\mathbf{K}_{II}^{-1} \mathbf{K}_{IJ} \\ \mathbf{I}_{JC} \end{bmatrix}, \quad (32)$$

where Ψ_{IC} has dimension $n_I \times n_C$ and \mathbf{I}_{JC} has dimension $n_C \times n_C$.

Note that nonlinear constraint modes are not considered in the present study, for a few reasons. First, to do so would require additional steps involving the derivation of another set of master-slave relations to describe nonlinear constraint modes (even if

they are static). Also, if one were to use nonlinear constraint modes in the synthesis procedure, the coefficients of the nonlinear terms would be functions of the constraint mode amplitudes, which would make the synthesis process cumbersome to the point of being impractical. Furthermore, and perhaps most importantly, since fixed-interface methods work best for assemblies of weakly coupled subsystems, for which fixed-interface (linear or nonlinear, as the case may be) modes are well-suited to describe component motion accurately, it seems appropriate to use linear constraint modes to represent the small interface-induced motion in the components.

Equations (20) and (21) are transformed into linear modal coordinates using equations (24) and (25). The equations of motion for both substructures expressed in terms of these coordinates are given by

$$\begin{bmatrix} \mathbf{I}_{NN} & \mathbf{M}_{NC} \\ \mathbf{M}_{CN} & \mathbf{M}_{CC} \end{bmatrix}^\alpha \begin{bmatrix} \ddot{\eta}_N \\ \ddot{\eta}_C \end{bmatrix}^\alpha + \begin{bmatrix} \Lambda_{NN} & \mathbf{0} \\ \mathbf{0} & \mathbf{K}_{CC} \end{bmatrix}^\alpha \begin{bmatrix} \eta_N \\ \eta_C \end{bmatrix}^\alpha + \begin{bmatrix} \tilde{\mathbf{G}}_N(\eta_N, \eta_C) \\ \tilde{\mathbf{G}}_C(\eta_N, \eta_C) \end{bmatrix}^\alpha = \begin{bmatrix} \mathbf{0} \\ \mathbf{F}_C \end{bmatrix}^\alpha \quad (33)$$

$$\begin{bmatrix} \mathbf{I}_{NN} & \mathbf{M}_{NC} \\ \mathbf{M}_{CN} & \mathbf{M}_{CC} \end{bmatrix}^\beta \begin{bmatrix} \ddot{\eta}_N \\ \ddot{\eta}_C \end{bmatrix}^\beta + \begin{bmatrix} \Lambda_{NN} & \mathbf{0} \\ \mathbf{0} & \mathbf{K}_{CC} \end{bmatrix}^\beta \begin{bmatrix} \eta_N \\ \eta_C \end{bmatrix}^\beta + \begin{bmatrix} \tilde{\mathbf{G}}_N(\eta_N, \eta_C) \\ \tilde{\mathbf{G}}_C(\eta_N, \eta_C) \end{bmatrix}^\beta = \begin{bmatrix} \mathbf{0} \\ \mathbf{F}_C \end{bmatrix}^\beta, \quad (34)$$

with junction boundary conditions on the displacements and forces:

$$\mathbf{X}_J^\alpha = \eta_C^\alpha = \eta_C^\beta = \mathbf{X}_J^\beta, \quad (35)$$

$$\mathbf{F}_C^\alpha = \mathbf{F}_J^\alpha \text{ and } \mathbf{F}_C^\beta = \mathbf{F}_J^\beta \quad (36)$$

$$\mathbf{F}_C^\alpha + \mathbf{F}_C^\beta = \mathbf{0}. \quad (37)$$

We now turn to the synthesis procedure.

3.3 Synthesis with Nonlinear Modal Reduction

In this section, the model size of the substructures is reduced using the NNM constraint relations. The substructure ROMs are then synthesized to obtain the final ROM that describes the dynamics of the combined structure.

Again, the superscripts α and β are omitted in the derivation. The component forms of equations (33) and (34) are given by

$$\ddot{\eta}_i^N + \sum_{s=1}^{n_C} m_{is}^{NC} \ddot{\eta}_s^C + \omega_i^2 \eta_i^N + \tilde{g}_i^N(\eta_l^N, \eta_k^N, \eta_r^C) = 0 \quad (38)$$

$$\ddot{\eta}_k^N + \sum_{s=1}^{n_C} m_{ks}^{NC} \ddot{\eta}_s^C + \omega_k^2 \eta_k^N + \tilde{g}_k^N(\eta_l^N, \eta_k^N, \eta_r^C) = 0 \quad (39)$$

$$\begin{aligned} \sum_{j=1}^n m_{rj}^{CN} \ddot{\eta}_j^N + \sum_{s=1}^{n_C} m_{rs}^{CC} \ddot{\eta}_s^C + \sum_{s=1}^{n_C} k_{rs}^{CC} \eta_s^C \\ + \tilde{g}_r^C(\eta_l^N, \eta_k^N, \eta_r^C) = F_r^J, \end{aligned} \quad (40)$$

$$\begin{aligned} \text{for } i, l = 1, 2, 3, \dots, n, \quad i, l \neq k; \\ r = 1, 2, 3, \dots, n_C, \end{aligned}$$

where k is the k^{th} fixed-interface master mode defined in section 3.2.1. From equation (38), the expression for $\ddot{\eta}_i^N$ is obtained, and it is used in equation (40). Rearranging and grouping terms in equation (40) yields

$$\begin{aligned} m_{rk}^{CN} \ddot{\eta}_k^N + \sum_{s=1}^{n_C} m_{rs}^{CC, \text{update}} \ddot{\eta}_s^C + \sum_{s=1}^{n_C} k_{rs}^{CC} \eta_s^C \\ + \tilde{g}_r^{C, \text{update}}(\eta_l^N, \eta_k^N, \eta_r^C) = F_r^J \end{aligned} \quad (41)$$

$$\text{where } m_{rs}^{CC, \text{update}} = m_{rs}^{CC} + m_{rs}^{CC, *}, \quad (42)$$

$$\text{and } m_{rs}^{CC, *} = \sum_{j=1, j \neq k}^n -m_{rj}^{CN} m_{js}^{NC}, \quad (43)$$

$$\text{and } \tilde{g}_r^{C, \text{update}} = \tilde{g}_r^C + \tilde{g}_r^{C, *}, \quad (44)$$

$$\text{and } \tilde{g}_r^{C, *} = \sum_{j=1, j \neq k}^n m_{rj}^{CN} (-\omega_j^2 \eta_j^N - \tilde{g}_j^N), \quad (45)$$

$$\text{for } r = 1, 2, 3, \dots, n_C.$$

The modal constraints given in equation (30) are used in equations (39) and (41) to reduce the equations of motion associated with the synthesized fixed-interface linear modal coordinates (which are coupled to the constraint modes) onto the k^{th} fixed-interface NNM invariant manifold (which is uncoupled from the constraint modes). This approximation will yield an accurate ROM if substructures α and β are weakly coupled, that is, the actual NNM invariant manifold of dimension $2 \times (2 + n_C)$ of the whole structure remains close to the k^{th} fixed-interface NNM invariant manifolds of the substructures, which are of dimension 2×2 . Note that the fixed-interface master modes of the substructures need not be the same.

With the NNM reduction of substructures α and β , equations (39) and (41) can be expressed in matrix form as

$$\begin{bmatrix} 1 & \mathbf{M}_{\text{KC}} \\ \mathbf{M}_{\text{CK}} & \mathbf{M}_{\text{CC}}^{\text{update}} \end{bmatrix}^{\alpha} \begin{bmatrix} \ddot{\eta}_k \\ \ddot{\eta}_c \end{bmatrix}^{\alpha} + \begin{bmatrix} \omega_k^2 & \mathbf{0} \\ \mathbf{0} & \mathbf{K}_{\text{CC}} \end{bmatrix}^{\alpha} \begin{bmatrix} \eta_k \\ \eta_c \end{bmatrix}^{\alpha} + \begin{bmatrix} \tilde{\mathbf{G}}_k(\eta_k, \dot{\eta}_k, \eta_c) \\ \tilde{\mathbf{G}}_c^{\text{update}}(\eta_k, \dot{\eta}_k, \eta_c) \end{bmatrix}^{\alpha} = \begin{bmatrix} 0 \\ \mathbf{F}_J \end{bmatrix}^{\alpha} \quad (46)$$

$$\begin{bmatrix} 1 & \mathbf{M}_{\text{KC}} \\ \mathbf{M}_{\text{CK}} & \mathbf{M}_{\text{CC}}^{\text{update}} \end{bmatrix}^{\beta} \begin{bmatrix} \ddot{\eta}_k \\ \ddot{\eta}_c \end{bmatrix}^{\beta} + \begin{bmatrix} \omega_k^2 & \mathbf{0} \\ \mathbf{0} & \mathbf{K}_{\text{CC}} \end{bmatrix}^{\beta} \begin{bmatrix} \eta_k \\ \eta_c \end{bmatrix}^{\beta} + \begin{bmatrix} \tilde{\mathbf{G}}_k(\eta_k, \dot{\eta}_k, \eta_c) \\ \tilde{\mathbf{G}}_c^{\text{update}}(\eta_k, \dot{\eta}_k, \eta_c) \end{bmatrix}^{\beta} = \begin{bmatrix} 0 \\ \mathbf{F}_J \end{bmatrix}^{\beta}, \quad (47)$$

along with the junction boundary conditions from equations (35) and (37). The final form of the synthesized ROM is obtained by imposing the junction conditions, equations (35) and (37), on equations (46) and (47), resulting in

$$\begin{bmatrix} 1 & 0 & \mathbf{M}_{\text{KC}}^{\alpha} \\ 0 & 1 & \mathbf{M}_{\text{KC}}^{\beta} \\ \mathbf{M}_{\text{CK}}^{\alpha} & \mathbf{M}_{\text{CK}}^{\beta} & \mathbf{M}_{\text{CC}}^{\text{update}} \end{bmatrix} \begin{bmatrix} \ddot{\eta}_k^{\alpha} \\ \ddot{\eta}_k^{\beta} \\ \ddot{\eta}_c \end{bmatrix} + \begin{bmatrix} (\omega_k^{\alpha})^2 & 0 & \mathbf{0} \\ 0 & (\omega_k^{\beta})^2 & \mathbf{0} \\ \mathbf{0} & \mathbf{0} & \mathbf{K}_{\text{CC}} \end{bmatrix} \begin{bmatrix} \eta_k^{\alpha} \\ \eta_k^{\beta} \\ \eta_c \end{bmatrix} + \begin{bmatrix} \tilde{\mathbf{G}}_k^{\alpha} \\ \tilde{\mathbf{G}}_k^{\beta} \\ \tilde{\mathbf{G}}_c^{\text{update}} \end{bmatrix} = \begin{bmatrix} 0 \\ 0 \\ \mathbf{0} \end{bmatrix}, \quad (48)$$

$$\text{where } \mathbf{M}_{\text{CC}}^{\text{update}} = (\mathbf{M}_{\text{CC}}^{\text{update},\alpha} + \mathbf{M}_{\text{CC}}^{\text{update},\beta}), \quad (49)$$

$$\text{and } \mathbf{K}_{\text{CC}} = (\mathbf{K}_{\text{CC}}^{\alpha} + \mathbf{K}_{\text{CC}}^{\beta}), \quad (50)$$

$$\text{and } \tilde{\mathbf{G}}_c^{\text{update}} = \tilde{\mathbf{G}}_c^{\text{update},\alpha}(\eta_k^{\alpha}, \dot{\eta}_k^{\alpha}, \eta_c) + \tilde{\mathbf{G}}_c^{\text{update},\beta}(\eta_k^{\beta}, \dot{\eta}_k^{\beta}, \eta_c). \quad (51)$$

In summary, this nonlinear CMS process involves two steps of model reduction, one of which is standard and uses linear modes, while the other involves the NNMs. First, we use the linear modal reduction described in section 3.2 to reduce the system DOF from $(n_I^{\alpha} + n_I^{\beta} + n_C)$ to $(n^{\alpha} + n^{\beta} + n_C)$. Note that this reduction is not central to the technique, and may not be used in some systems (in fact, it is not done in the example considered in the next section). Then, the key step makes use of the nonlinear modal reduction based on the approach described in sections 1 and 2, which reduces the system size from $(n^{\alpha} + n^{\beta} + n_C)$

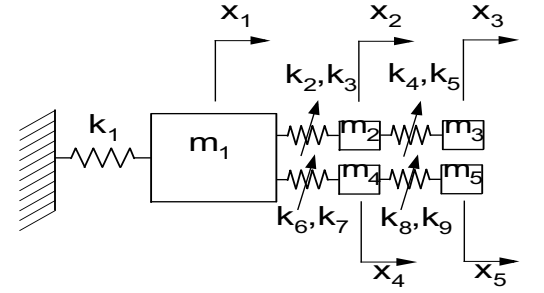


Figure 1. A five-degree of freedom spring-mass system.

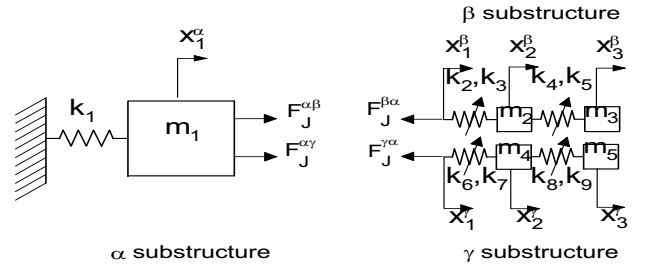


Figure 2. System substructures.

to $(2 + n_C)$ DOFs. Also, note that all these procedures can be and have been computationally automated. Therefore, it is quite practical to interface this fixed-interface nonlinear CMS with nonlinear finite element models of the form in equations (20) and (21).

4 APPLICATIONS

A five-DOF nonlinear spring-mass system is used as a “proof of concept” example that demonstrates the procedures and shows the effectiveness of the proposed method. The system is schematically depicted in Figure 1, and naturally partitions into the three substructures shown in Figure 2. The general features of this system are that the coupling mass m_1 is connected to ground

with a very stiff spring k_1 , such that its isolated natural frequency is significantly larger than the fixed-interface natural frequencies of the two attached subsystems (that is, when they are attached to ground instead of to m_1). In such a case, mass m_1 will have a relatively small amplitude for typical responses, and the fixed-interface modes of the two attached subsystems will be strongly reflected in the modes of the combined system. Thus, the procedure consists in developing single-DOF fixed-interface NNMs for the attached subsystems, and combining these using the proposed method, resulting in a three-DOF nonlinear ROM that captures the dynamics, except for the high-frequency modes of the two attached subsystems. However, by using NNMs to describe the subsystems, the essential nonlinear interactions between the linear modes in the substructures will be contained in the resulting ROM.

The equations of motion of the five-DOF spring-mass system are given by

$$\begin{bmatrix} m_1 & 0 & 0 & 0 & 0 \\ 0 & m_2 & 0 & 0 & 0 \\ 0 & 0 & m_3 & 0 & 0 \\ 0 & 0 & 0 & m_4 & 0 \\ 0 & 0 & 0 & 0 & m_5 \end{bmatrix} \begin{bmatrix} \ddot{x}_1 \\ \ddot{x}_2 \\ \ddot{x}_3 \\ \ddot{x}_4 \\ \ddot{x}_5 \end{bmatrix} + \begin{bmatrix} (k_1 + k_2 + k_6) & -k_2 & 0 & -k_6 & 0 \\ -k_2 & (k_2 + k_4) & -k_4 & 0 & 0 \\ 0 & -k_4 & k_4 & 0 & 0 \\ -k_6 & 0 & 0 & (k_6 + k_8) & -k_8 \\ 0 & 0 & 0 & -k_8 & k_8 \end{bmatrix} \begin{bmatrix} x_1 \\ x_2 \\ x_3 \\ x_4 \\ x_5 \end{bmatrix} + \begin{bmatrix} -k_3(x_2 - x_1)^3 - k_7(x_4 - x_1)^3 \\ k_3(x_2 - x_1)^3 - k_5(x_3 - x_2)^3 \\ k_5(x_3 - x_2)^3 \\ k_7(x_4 - x_1)^3 - k_9(x_5 - x_4)^3 \\ k_9(x_5 - x_4)^3 \end{bmatrix} = \begin{bmatrix} 0 \\ 0 \\ 0 \\ 0 \\ 0 \end{bmatrix}. \quad (52)$$

The equations of motion for the individual substructures and the junction boundary conditions are given by

$$m_1 \ddot{x}_1^\alpha + k_1 x_1^\alpha = F_J^{\alpha\beta} + F_J^{\alpha\gamma} \quad (53)$$

$$\begin{bmatrix} 0 & 0 & 0 \\ 0 & m_2 & 0 \\ 0 & 0 & m_3 \end{bmatrix} \begin{bmatrix} \ddot{x}_1^\beta \\ \ddot{x}_2^\beta \\ \ddot{x}_3^\beta \end{bmatrix} + \begin{bmatrix} k_2 & -k_2 & 0 \\ -k_2 & (k_2 + k_4) & -k_4 \\ 0 & -k_4 & k_4 \end{bmatrix} \begin{bmatrix} x_1^\beta \\ x_2^\beta \\ x_3^\beta \end{bmatrix} + \begin{bmatrix} -k_3(x_2^\beta - x_1^\beta)^3 \\ k_3(x_2^\beta - x_1^\beta)^3 - k_5(x_3^\beta - x_2^\beta)^3 \\ k_5(x_3^\beta - x_2^\beta)^3 \end{bmatrix} = \begin{bmatrix} F_J^{\beta\alpha} \\ 0 \\ 0 \end{bmatrix} \quad (54)$$

$$\begin{bmatrix} 0 & 0 & 0 \\ 0 & m_4 & 0 \\ 0 & 0 & m_5 \end{bmatrix} \begin{bmatrix} \ddot{x}_1^\gamma \\ \ddot{x}_2^\gamma \\ \ddot{x}_3^\gamma \end{bmatrix} + \begin{bmatrix} k_6 & -k_6 & 0 \\ -k_6 & (k_6 + k_8) & -k_8 \\ 0 & -k_8 & k_8 \end{bmatrix} \begin{bmatrix} x_1^\gamma \\ x_2^\gamma \\ x_3^\gamma \end{bmatrix} + \begin{bmatrix} -k_7(x_2^\gamma - x_1^\gamma)^3 \\ k_7(x_2^\gamma - x_1^\gamma)^3 - k_9(x_3^\gamma - x_2^\gamma)^3 \\ k_9(x_3^\gamma - x_2^\gamma)^3 \end{bmatrix} = \begin{bmatrix} F_J^{\gamma\alpha} \\ 0 \\ 0 \end{bmatrix} \quad (55)$$

$$x_1^\alpha = x_1^\beta = x_1^\gamma \quad (56)$$

$$F_J^{\alpha\beta} + F_J^{\beta\alpha} = 0 \quad (57)$$

$$F_J^{\alpha\gamma} + F_J^{\gamma\alpha} = 0. \quad (58)$$

The system parameters used for this study are $m_1 = 5, m_2 = 1, m_3 = 1, m_4 = 1, m_5 = 1, k_1 = 50, k_2 = 1, k_3 = 2, k_4 = 5, k_5 = 1, k_6 = 4, k_7 = 1, k_8 = 45$, and $k_9 = 1$.

The natural frequency of substructure α is $\omega^\alpha = 3.16$ rad/s, the first (linear) natural frequency of substructure β is $\omega_1^\beta = 0.69$ rad/s, and the first (linear) natural frequency of substructure γ is $\omega_1^\gamma = 1.40$ rad/s. Therefore the substructures β and γ are coupled through substructure α via weak coupling, since $\omega^\alpha \gg \omega_1^\beta, \omega_1^\gamma$.

Applying the procedures from section 3.2.1, the fixed-interface nonlinear mode manifolds for the fundamental modes of substructures β and γ are obtained. In this simple case the manifolds can be expressed as constraint functions in which the second linear modal amplitude and velocity for a substructure depend on the first modal amplitude and velocity of that substructure. The results obtained numerically for the modal amplitude functions are shown in figures (3) and (4). Note that there are similar surfaces obtained for the slaved modal velocities, although they are not shown here.

Then, applying the procedures from section 3.3, a nonlinear three-DOF ROM is obtained. In this case it describes the motion of the coupling mass and the first NNM for each of the attached substructures. This model is simulated with initial conditions

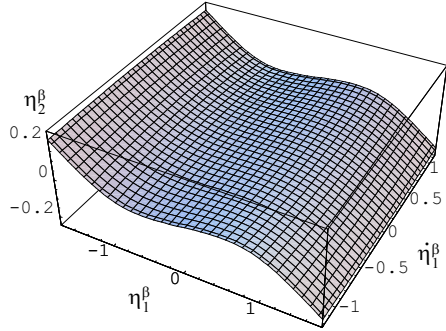


Figure 3. The contribution of the second fixed-interface linear mode amplitude $\eta_2^\beta = X_2^\beta(\eta_1^\beta, \dot{\eta}_1^\beta)$ to the first fixed-interface nonlinear mode manifold of substructure β .

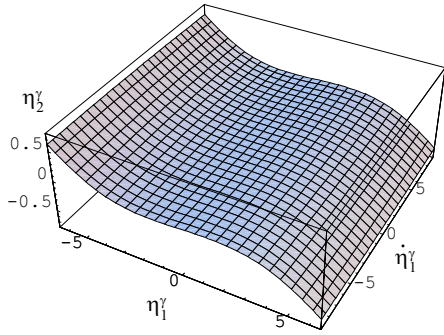


Figure 4. The contribution of the second fixed-interface linear mode amplitude $\eta_2^\gamma = X_2^\gamma(\eta_1^\gamma, \dot{\eta}_1^\gamma)$ to the first fixed-interface nonlinear mode manifold of substructure γ .

initiated on the first fixed-interface nonlinear mode manifolds of substructures β and γ , as follows: $\eta_1^\beta = 1.5, \eta_1^\gamma = 0.4$, and $\eta_C = 0.1$, with initial modal velocities taken to be zero.

For comparison purposes we use four models constructed in various manners. They are: the original five-DOF nonlinear model given in equation (52), a three-DOF nonlinear model obtained using linear CMS (that is, by projecting the nonlinear subsystem onto the fixed-interface linear mode and the linear constraint mode), a three-DOF linear model obtained using linear

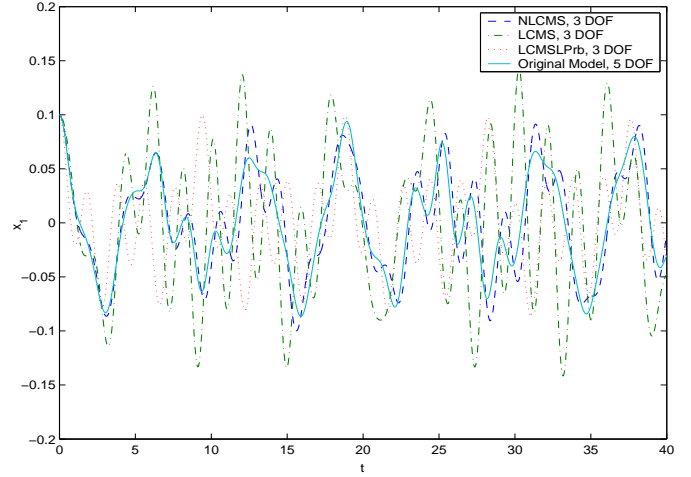


Figure 5. The time response of the displacement x_1 of mass m_1 from figure 1, which corresponds to x_1^α, x_1^β , and x_1^γ from figure 2.

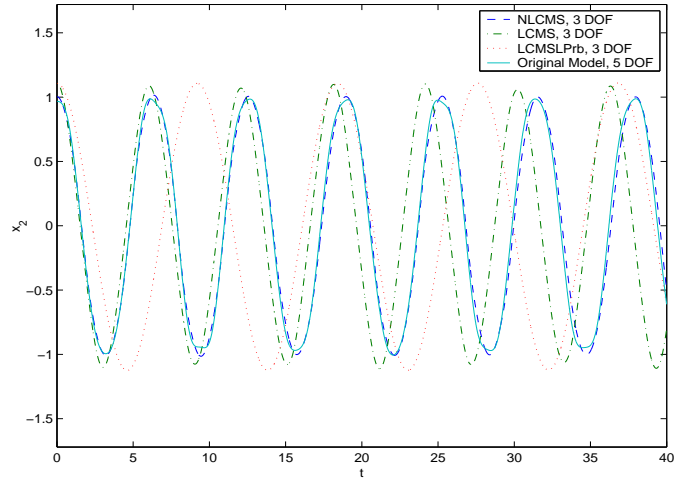


Figure 6. The time response of the displacement x_2 from figure 1, which corresponds to x_2^β from figure 2.

CMS (this is the linearized version of the previous model), and the three-DOF nonlinear CMS model developed by the proposed approach. Figures (5) to (9) depict the comparison of the time responses of the various physical degrees of freedom obtained by simulations of these four models. In these figures the dashed line labeled NLCMS corresponds to the three-DOF nonlinear CMS model, the dash-dot line labeled LCMS corresponds to the three-DOF nonlinear model obtained using linear CMS, the dotted line labeled LCMSLPrb corresponds to the three-DOF linear model obtained using linear CMS, and the solid line labeled Original Model corresponds to the five-DOF original model. From the

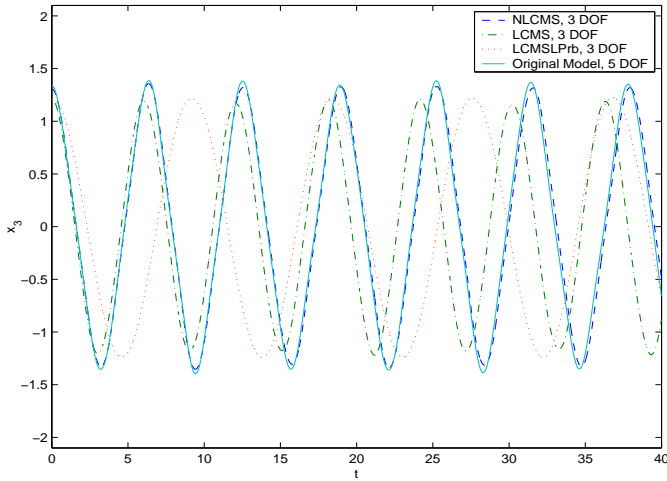


Figure 7. The time response of the displacement x_3 from figure 1, which corresponds to x_3^B from figure 2.

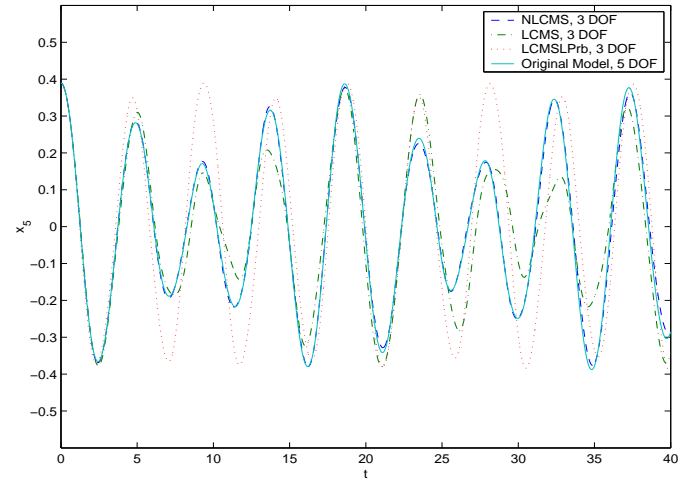


Figure 9. The time response of the displacement x_5 from figure 1, which corresponds to x_5^Y from figure 2.

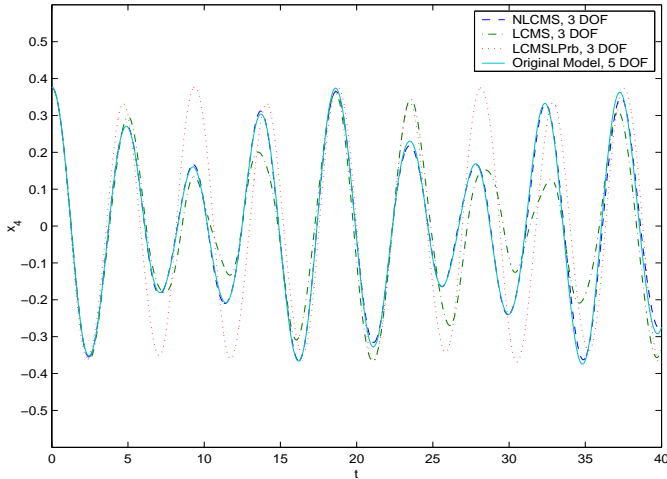


Figure 8. The time response of the displacement x_4 from figure 1, which corresponds to x_2^Y from figure 2.

simulation results it is clear that the fixed-interface nonlinear CMS model outperforms the other low-order models, including the linear CMS model, which is what is most commonly used in this type of problems.

It should be noted that there is a range of system parameters where this method gives satisfactory results. One particular trend worth noting is obtained by varying the stiffness k_1 . As k_1 is reduced to approach the same order as the stiffnesses of the substructures, the fixed-interface approximation begins to break down and the accuracy of the nonlinear CMS model deteriorates. On the other hand, as k_1 is increased, the nonlinear CMS model

becomes more accurate, but the amount of substructure interaction is reduced, leading to a system which consists of essentially decoupled motions for the two attached substructures. In this case, the coupling mass m_1 responds in a quasi-static manner to the forces applied at the interface by the attached substructures.

5 CONCLUSIONS

In this paper, we have shown how to extend the fixed-interface linear CMS technique of Craig and Bampton ([3]) to nonlinear structures by making use of fixed-interface NNMs in place of fixed-interface LNMs. This approach allows one to build nonlinear reduced-order models with improved accuracy for systems that are composed of assemblies of substructures. The example system presented here is quite simple, and the model reduction is not very significant (from five to three DOFs), but the method is suitable for more significant reductions, for example for industrial structures. This follows from the fact that the NNM method has been developed to the point where it can be applied to systems with thousands of DOFs. Current work is focusing on systems with many more DOFs, and includes substructures that are modeled by nonlinear FE techniques. Specifically, the case of rotating beams coupled through an elastic hub is under consideration, where each rotating beam and the hub are considered as substructures.

ACKNOWLEDGMENT

This work has been supported by a grant from the Army Research Office, with Dr. Gary Anderson as the grant monitor.

REFERENCES

- [1] Hurty, W. C., 1960, "Vibration of Structural Systems by Component Mode Synthesis," *Proceedings of the American Society of Civil Engineers*, **85**(4), pp. 51-69.
- [2] Hurty, W.C., 1965, "Dynamic Analysis of Structural Systems Using Component Modes," *AIAA Journal*, **3**(4), pp. 678-685.
- [3] Craig, R. R. and Bampton, M. C. C., 1968, "Coupling of Substructures for Dynamic Analyses," *AIAA Journal*, **6**(7), pp. 1313-1319.
- [4] Craig, R. R., 1995, "Substructure Methods in Vibration," *Journal of Mechanical Design*, **117**, pp. 207-213.
- [5] Seshu, P., 1997, "Review Substructuring and Component Mode Synthesis," *Shock and Vibration*, **4**(3), pp. 199-210.
- [6] Bamford, R., Wada, B. K., Garba, J. A., and Chisholm, J., 1971, "Dynamic Analysis of Large Structural Systems," *Synthesis of Vibrating Systems, ASME Booklet*, pp. 57-71.
- [7] Goldenberg, S., and Shapiro, M., 1972, "A Study of Modal Coupling Procedures for the Space Shuttle," *NASA Contractor Report 112252, Grumman Aerospace Corp.*
- [8] Spanos, J. T., and Tsuha, W. S., 1991, "Selection of Component Modes for Flexible Multibody Simulation," *Journal of Guidance, Control, and Dynamics*, **14**(2), pp. 278-286.
- [9] Farhat, C., and Geradin, M., 1994, "On A Component Mode Synthesis Method and Its Application to Incompatible Substructures," *Computers Structures*, **51**(5), pp. 459-473.
- [10] Majed, A., and Spanos, P. D., 1997, "Nonlinear Dynamics of Structures Via Residual Flexibility of Components," *Journal of Aerospace Engineering*, **10**(4), pp. 173-178.
- [11] Noor, A. K., 1994, "Recent Advances and Applications of Reduction Methods," *Applied Mechanics Reviews*, **47**(5), pp. 125-146.
- [12] Shaw, S. W. and Pierre, C., 1993, "Normal modes for nonlinear vibratory systems," *Journal of Sound and Vibration*, **164**(1), pp. 85-124.
- [13] Shaw, S. W. and Pierre, C., 1994, "Normal modes of vibration for non-linear continuous systems," *Journal of Sound and Vibration*, **169**(3), pp. 319-347.
- [14] Shaw, S. W., Pierre, C., and Pesheck, E., 1999, "Modal analysis-based reduced-order models for nonlinear structures-an invariant manifold approach," *The Shock and Vibration Digest*, **31**(1), pp. 3-16.
- [15] Pesheck, E., Pierre, C., and Shaw, S. W., 2002a, "Model reduction of a nonlinear rotating beam through nonlinear normal modes," *Journal of Vibration and Acoustics*, **124**, pp. 229-236.
- [16] Pesheck, E., Pierre, C., and Shaw, S. W., 2002b, "A new Galerkin-based approach for accurate nonlinear normal modes through invariant manifolds," *Journal of Sound and Vibration*, **249**(5), pp. 971-993.
- [17] Pesheck, E., Pierre, C., and Shaw, S. W., 2001, "Accurate reduced order models for a simple rotor blade model using nonlinear normal modes," *Mathematical and Computer Modelling*, **33**, pp. 1085-1097.
- [18] Apiwattanalungarn, P., Shaw, S. W., Pierre, C., and Jiang, D., 2003, "Finite-Element-Based Nonlinear Modal Reduction of a Rotating Beam with Large-Amplitude Motion," *Journal of Vibration and Control*, **9**(3-4), pp. 235-263.